# Orientation Estimation Using a Quaternion-Based Indirect Kalman Filter With Adaptive Estimation of External Acceleration

Young Soo Suh, *Member, IEEE*

***Abstract*—This paper is concerned with orientation estimation using inertial and magnetic sensors. A quaternion-based indirect Kalman filter structure is used. The magnetic sensor output is only used for yaw angle estimation using two-step measurement updates. External acceleration is estimated from the residual of the filter and compensated by increasing the measurement noise covariance. Using the direction information of external information, the proposed method prevents unnecessarily increasing the measurement noise covariance corresponding to the accelerometer output, which is not affected by external acceleration. Through numerical examples, the proposed method is verified.**

***Index Terms*—Adaptive filters, inertial sensors, Kalman filtering, orientation estimation, quaternion.**

## I. Introduction

ORIENTATION estimation (pitch, roll, and yaw angles) is used in many applications: motion tracker [1], unmanned aerial vehicles [2], and biomedical applications [3]. One of increasingly popular approaches is using inertial and magnetic sensors to estimate orientation. A typical system consists of a triaxial gyroscope (to measure angular velocity), a triaxial accelerometer (to measure gravity), and a triaxial magnetic sensor (to measure the Earth's magnetic field).

If the initial estimation is given, orientation can be computed by integrating the gyroscope output. Its estimation error, however, will diverge due to gyroscope bias and numerical integration errors. On the other hand, orientation can also be computed using the accelerometer and the magnetic sensor output. The estimation error, in this case, could become large due to external acceleration and magnetic disturbance. Thus, the fundamental issue in every orientation estimation algorithm is how to combine the gyroscope, the accelerometer, and the magnetic sensor output.

In this paper, a quaternion-based indirect Kalman filter is proposed. The gyroscope output is integrated to compute orientation. Quaternion instead of Euler angles is used because of its singularity-free orientation representation [4], [5]. The error in this orientation is then estimated using a Kalman filter, where the accelerometer and the magnetic sensor output are used. Since the orientation error is estimated instead of directly estimating orientation, it is called an indirect filter [6], [7]. The advantage of an indirect filter is that the state dimension is smaller and its response is fast. The orientation error is represented by a multiplication to the computed quaternion, and the multiplicative extended Kalman filter is used. We note that this quaternion multiplication was used in [8]–[10].

The two contributions of the proposed method are as follows: 1) a new method of orientation computation from the magnetic sensor and 2) an adaptive method compensating the external acceleration effect.

With regard to the first contribution, we note that the magnetic sensor output provides not only yaw information but also some information on pitch and roll angles. In [11] and [12], pitch, roll, and yaw angles are computed using the magnetic sensor output: both pitch and roll angles cannot be computed, but some information on pitch and roll can be obtained. One critical drawback is that pitch and roll angles are affected by magnetic disturbance. Since there is large magnetic disturbance indoors, there is a tendency that pitch and roll errors become large when the method is used indoors. Thus, using the magnetic sensor output only to compute the yaw angle is more widely used [7], [13], [14], where it is not directly applicable to a quaternion-based indirect Kalman filter. In this paper, a standard Kalman filter is modified so that the magnetic sensor output is only used for yaw estimation error compensation.

With regard to the second contribution, an adaptive method to deal with external acceleration is considered. When there is no external acceleration, the accelerometer output provides accurate pitch and roll angles. When there is external acceleration, this is not the case. Thus, smaller weights should be given to the accelerometer output with respect to the gyroscope output when there is external acceleration. In [11], [15], and [16], if the norm of the accelerometer output is not near 9.8 $m/s^2$ (gravitational acceleration), it is determined that there is external acceleration, and smaller weights are given to the accelerometer output by increasing the corresponding measurement noise covariance. An alternative method is proposed, where external acceleration is directly estimated from the filter residual. The proposed adaptive method is a slight modification of the general adaptive Kalman filter algorithm in [17, Ch. 10].

The main advantage of the proposed method is that the direction of external acceleration is estimated and used for

Manuscript received August 12, 2009; revised January 29, 2010; accepted January 30, 2010. Date of publication May 10, 2010; date of current version November 10, 2010. This work was supported by the National Research Foundation of Korea, Korean Government, under Grant 2009-0074773. The Associate Editor coordinating the review process for this paper was Dr. Salvatore Baglio.

The author is with the Department of Electrical Engineering, University of Ulsan, Ulsan 680-749, Korea (e-mail: yssuh@ulsan.ac.kr).

Color versions of one or more of the figures in this paper are available online at http://ieeexplore.ieee.org.

Digital Object Identifier 10.1109/TIM.2010.2047157

compensation. For example, suppose there is external acceleration only in the $x$-direction. In the accelerometer norm-based method, smaller weights are given to all three-axis accelerometer output, and thus, the valuable information contained in the $y$- and $z$-axis accelerometer output is lost. In the proposed method, smaller weights are only given to the $x$-axis accelerometer output, and thus, the $y$- and $z$-axis accelerometer output is still used in the filter.

This paper is organized as follows: In Section II, basic equations of a quaternion-based indirect Kalman filter is given. In Section III, a two-step measurement update method is proposed, where the magnetic sensor is only used for yaw angle estimation. In Section IV, an adaptive algorithm compensating external acceleration is proposed. Numerical examples and conclusion are given in Sections V and VI, respectively.

## II. Quaternion-Based Indirect Kalman Filter

Two coordinate frames (body frame and navigation frame) are used. The body frame $(x_b, y_b, z_b)$ has its origin at the triaxial gyroscope, and each axis points along each of the gyroscope axis. The navigation frame $(x_n, y_n, z_n)$ is a local-level frame with its axes pointing north, east, and up. A quaternion $q = [\,q_0 \quad q_1 \quad q_2 \quad q_3\,]' \in R^4$ is used to denote the orientation quaternion in the navigation frame. Note that $p_n$ (a point in the navigation frame) and $p_b$ (a point in the body frame) are related as follows:

$$p_b = C(q)p_n$$

where the rotation matrix $C(q)$ is defined by

$$C(q) \triangleq \begin{bmatrix} 2q_0^2 + 2q_1^2 - 1 & 2q_1q_2 + 2q_0q_3 & 2q_1q_3 - 2q_0q_2 \\ 2q_1q_2 - 2q_0q_3 & 2q_0^2 + 2q_2^2 - 1 & 2q_2q_3 + 2q_0q_1 \\ 2q_1q_3 + 2q_0q_2 & 2q_2q_3 - 2q_0q_1 & 2q_0^2 + 2q_3^2 - 1 \end{bmatrix}. \tag{1}$$

The orientation estimation problem in this paper is to estimate quaternion $q$. The derivative of $q$ is given by the following equation [18]:

$$\dot{q} = \frac{1}{2} q \otimes \omega \tag{2}$$

where $\omega \in R^3$ is the angular velocity, and $\otimes$ represents quaternion multiplication.

The accelerometer output $y_a$, the gyroscope output $y_g$, and the magnetic sensor output $y_m$ are given by

$$\begin{aligned} y_a &= C(q)\tilde{g} + b_a + v_a + a_b \\ y_g &= \omega + b_g + v_g \\ y_m &= C(q)\tilde{m} + v_m. \end{aligned} \tag{3}$$

Symbols $\tilde{g}$ and $\tilde{m}$ are defined by

$$\tilde{g} \triangleq \begin{bmatrix} 0 \\ 0 \\ g \end{bmatrix} \quad \tilde{m} \triangleq \begin{bmatrix} \cos\alpha \\ 0 \\ -\sin\alpha \end{bmatrix}$$

where $g$ is the gravitational acceleration, and $\alpha$ is the dip angle [19]. Sensor noises $v_a$, $v_g$, and $v_m$ are assumed to be zero-mean white Gaussian noises satisfying

$$\begin{aligned} \mathrm{E}\{v_a(t)v_a(s)'\} &= R_a\delta(t-s) \\ \mathrm{E}\{v_g(t)v_g(s)'\} &= R_g\delta(t-s) \\ \mathrm{E}\{v_m(t)v_m(s)'\} &= R_m\delta(t-s) \\ \mathrm{E}\{v_a(t)v_m(s)'\} &= 0 \\ \mathrm{E}\{v_a(t)v_g(s)'\} &= 0 \\ \mathrm{E}\{v_m(t)v_g(s)'\} &= 0. \end{aligned}$$

Accelerometer bias $b_a$ and gyroscope bias $b_g$ are assumed to be nearly constant, and $a_b$ represents unknown external acceleration.

### A. Indirect Kalman Filter

The objective of a filter is to estimate $q$ from $y_a$, $y_g$, and $y_m$. In this paper, we will use an indirect Kalman filter. First, a quaternion estimate $\hat{q}$ is computed from the following equation:

$$\frac{d\hat{q}}{dt} = \frac{1}{2}\hat{q} \otimes y_g. \tag{4}$$

Since $y_g \neq \omega$ (due to $v_g$ and $b_g$), $\hat{q} \neq q$, i.e., $\hat{q}$ contains an orientation error. We introduce $\tilde{q}_e$ to denote a small error in $\hat{q}$ [8]–[10] so that

$$q = \hat{q} \otimes \tilde{q}_e. \tag{5}$$

Note that $\tilde{q}_e$ does not depend on $\omega$ (angular velocity) but depends on gyroscope noise $v_g$ and gyroscope bias $b_g$, which can be assumed to be small. Thus, even if the rotations are large, we can assume that $\tilde{q}_e$ is small. Assuming $\tilde{q}_e$ is small, we can approximate $\tilde{q}_e$ as follows:

$$\tilde{q}_e \approx \begin{bmatrix} 1 \\ q_e \end{bmatrix}. \tag{6}$$

In an indirect Kalman filter, $\tilde{q}_e$ is estimated, and $q$ can be estimated using (5) instead of directly estimating $q$. From [9], we have

$$\dot{q}_e = \frac{1}{2}(\omega - y_g) + \frac{1}{2}q_e \times (\omega - y_g) - y_g \times q_e.$$

Assuming $q_e$ and $\omega - y_g$ are small, we can ignore the second term of the right-hand side: if $q_e$ and $\omega - y_g$ are small, $q_e \times (\omega - y_g)$ is very small and can be ignored. Thus, we have

$$\dot{q}_e \approx -y_g \times q_e - \frac{1}{2}(b_g + v_g). \tag{7}$$

Defining the state $x$ by

$$x = \begin{bmatrix} q_e \\ b_g \\ b_a \end{bmatrix} \in R^{9\times 1} \tag{8}$$

we have the following process equation for the Kalman filter:

$$\dot{x}(t) = Ax(t) + \begin{bmatrix} -0.5v_g \\ v_{b_g} \\ v_{b_a} \end{bmatrix} \tag{9}$$

where

$$A \triangleq \begin{bmatrix} -[y_g\times] & -0.5I & 0 \\ 0 & 0 & 0 \\ 0 & 0 & 0 \end{bmatrix}.$$

For a vector $p \in R^3$, $[p\times]$ is defined by

$$[p\times] \triangleq \begin{bmatrix} 0 & -p_3 & p_2 \\ p_3 & 0 & -p_1 \\ -p_2 & p_1 & 0 \end{bmatrix}.$$

Small process noises $v_{b_g}$ and $v_{b_a}$ are added so that the bias estimation is not stopped soon. If $v_{b_g} = 0$ and $v_{b_a} = 0$, the error covariance of the filter corresponding to state $b_g$ and $b_a$ will be very small after some time, and thus, no bias update is done afterward. We assume that

$$\mathrm{E}\left\{ \begin{bmatrix} -0.5v_g(t) \\ v_{b_g}(t) \\ v_{b_a}(t) \end{bmatrix} \begin{bmatrix} -0.5v_g(s) \\ v_{b_g}(s) \\ v_{b_a}(s) \end{bmatrix}' \right\} = Q\delta(t-s) \tag{10}$$

where

$$Q \triangleq \mathrm{Diag}\{0.25R_g, Q_{b_g}, Q_{b_a}\}.$$

Now, a measurement equation for an indirect Kalman filter is derived. From (5), we have

$$C(q) = C(\bar{q}_e)C(\hat{q}). \tag{11}$$

With (6), the rotation matrix $C(\bar{q}_e)$ is given by

$$C(\bar{q}_e) = \begin{bmatrix} 1+2q_{e,1}^2 & 2q_{e,1}q_{e,2}+2q_{e,3} & 2q_{e,1}q_{e,3}-2q_{e,2} \\ 2q_{e,1}q_{e,2}-2q_{e,3} & 1+2q_{e,2}^2 & 2q_{e,2}q_{e,3}+2q_{e,1} \\ 2q_{e,1}q_{e,3}+2q_{e,2} & 2q_{e,2}q_{e,3}-2q_{e,1} & 1+2q_{e,3}^2 \end{bmatrix}. \tag{12}$$

With the assumption that $q_{e,1}$, $q_{e,2}$, and $q_{e,3}$ are small, we can ignore the second-order terms: i.e., we assume $q_{e,i}q_{e,j} \approx 0$. Then, we have

$$C(\bar{q}_e) \approx \begin{bmatrix} 1 & 2q_{e,3} & -2q_{e,2} \\ -2q_{e,3} & 1 & 2q_{e,1} \\ 2q_{e,2} & -2q_{e,1} & 1 \end{bmatrix} = I - 2[q_e\times]. \tag{13}$$

Inserting (13) and (11) into (3), we have

$$\begin{aligned} y_a - C(\hat{q})\tilde{g} &= 2\left[C(\hat{q})\tilde{g}\times\right] q_e + a_b + v_a + b_a \\ y_m - C(\hat{q})\tilde{m} &= 2\left[C(\hat{q})\tilde{m}\times\right] q_e + v_m. \end{aligned} \tag{14}$$

While deriving (14), we have used the following fact:

$$[q_e\times]C(\hat{q})\tilde{g} = -\left[C(\hat{q})\tilde{g}\times\right] q_e.$$

Equations (9) and (14) constitute a system model for an indirect Kalman filter. Note that $y_a - C(\hat{q})\tilde{g}$ and $y_m - C(\hat{q})\tilde{m}$ are used as measurements to an indirect Kalman filter. The overall structure of the indirect Kalman filter is given in Fig. 1.

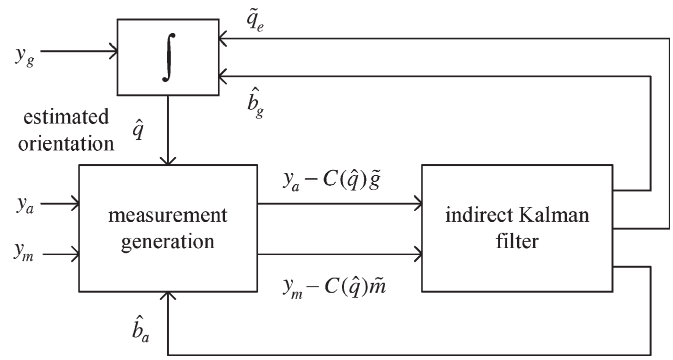


Fig. 1. Overview of the indirect Kalman filter.

### B. Discretization

The output (14) is assumed to be periodically sampled with the sampling period $T$. The discrete signal $x_k$ represents $x(kT)$. The system (9) is discretized as follows:

$$x_{k+1} = \phi_k x_k + w_k \tag{15}$$

where

$$\phi_k \triangleq \exp(AT)$$

$$Q_{d,k} \triangleq \mathrm{E}\{w_k w_k'\} = \int_{kT}^{(k+1)T} \exp(At)Q\exp(At)'\,dt.$$

Note that $\phi_k$ and $Q_{d,k}$ should be computed at every step since $A$ is time varying. In the real-time application, it could be computationally demanding to compute exact values of $\phi_k$ and $Q_{d,k}$. In this paper, the following simple approximation is used:

$$\begin{aligned} \phi_k &\approx I + A(kT)T + 0.5A(kT)^2T^2 \\ Q_{d,k} &\approx \int_{kT}^{(k+1)T} (I+At)Q(I+At)'\,dt \\ &= \int_{kT}^{(k+1)T} Q + AQt + QA't\,dt \\ &\approx QT + \frac{1}{2}A(kT)Q + \frac{1}{2}QA(kT)'. \end{aligned} \tag{16}$$

Based on the discrete model (15), a standard project ahead algorithm is used [6], i.e.,

$$\begin{aligned} \hat{x}_{k+1}^- &= \phi_k \hat{x}_k \\ P_{k+1}^- &= \phi_k P_k \phi_k' + Q_d \end{aligned} \tag{17}$$

where $\hat{x}_k^-$ and $\hat{x}_k$ are a state estimate before a measurement update and a state estimate after a measurement update, respectively. Estimation error covariances $P_k^-$ and $P_k$ are defined by

$$\begin{aligned} P_k^- &= \mathrm{E}\left\{ \left(x_k - \hat{x}_k^-\right)\left(x_k - \hat{x}_k^-\right)' \right\} \\ P_k &= \mathrm{E}\left\{ (x_k - \hat{x}_k)(x_k - \hat{x}_k)' \right\}. \end{aligned}$$

The quaternion integration equation (2) is approximated by a discrete equation, where the third-order local linearization algorithm is used (see [17, eq. (110)], i.e.,

$$\begin{aligned} q_{k+1} = \Bigg( I &+ \frac{3}{4}\Omega_k T - \frac{1}{4}\Omega_{k-1} T - \frac{1}{6}\|\omega_k\|_2^2 T^2 \\ &- \frac{1}{24}\Omega_k \Omega_{k-1} T^2 - \frac{1}{48}\|\omega_k\|_2^2 \Omega_k T^3 \Bigg) q_k. \end{aligned} \tag{18}$$

After the computation, the quaternion is normalized so that the unit constraint $\|q_{k+1}\| = 1$ is satisfied.

## III. Two-Step Measurement Updates

Magnetic disturbance sometimes could be very large. This is particularly true for indoor environments: computer, TV, and other electrical devices can cause large magnetic disturbances [20]. When the measurement equation (14) is used, magnetic disturbance affects not only yaw but also pitch and roll. A common approach is to use the magnetic sensor output only for yaw estimation. This can be done by computing $q_e$ from $y_a$ and $y_m$ using the TRIAD method [21] or the factored quaternion algorithm [13]. Then, the computed $q_e$ can be used as a measurement for the Kalman filter. However, important information, which could be used in the adaptive algorithm in Section IV, is lost in the algorithms.

In this section, we propose a two-step measurement update algorithm, which consists of an accelerometer measurement update and a magnetic sensor measurement update. In an accelerometer measurement update, $\hat{x}_k^-$ is updated using $y_a - C(\hat{q})\tilde{g}$, where the updated state is denoted by $\hat{x}_{a,k}$. Using the $q_e$ part in $\hat{x}_{a,k}$, $C(\hat{q})$ is updated as in (11). Then, the $q_e$ part of $\hat{x}_{a,k}$ (that is, the first three elements of $\hat{x}_{a,k}$) is set to zero.

In a magnetic sensor measurement update, $\hat{x}_{k,a}$ is updated to $\hat{x}_k$ using $y_m - C(\hat{q})\tilde{m}$, where $q_e$ is constrained so that the magnetic sensor output only affects the yaw angle.

- Accelerometer measurement update: $y_a - C(\hat{q})\tilde{g}$ is used to update $\hat{x}_k^-$. Thus

$$\begin{aligned} K_{a,k} &= P_k^- H_{a,k}' \left( H_{a,k} P_k^- H_{a,k}' + R_a + \hat{Q}_{a_b,k} \right)^{-1} \\ \hat{x}_{a,k} &= \hat{x}_k^- + K_{a,k}\left( z_{a,k} - H_{a,k}\hat{x}_k^- \right) \\ P_{a,k} &= (I - K_{a,k}H_{a,k}) P_k^- (I - K_{a,k}H_{a,k})' \\ &\quad + K_{a,k}\left( R_a + \hat{Q}_{a_b,k} \right) K_{a,k}' \end{aligned} \tag{19}$$

where

$$\begin{aligned} H_{a,k} &\triangleq \left[\, 2\,[C(\hat{q})\tilde{g}\times] \quad 0 \quad I \,\right] \\ z_{a,k} &\triangleq y_{a,k} - C(\hat{q}_k)\tilde{g}. \end{aligned}$$

All nine states of $\hat{x}_k^-$ are updated in this step. The estimated external acceleration covariance $\hat{Q}_{a_b,k}$ is explained in Section IV [see (34) and (35)].

- $C(\hat{q})$ is updated using $\hat{x}_k^-$. Thus

$$\begin{aligned} q_e &= \hat{x}_{a,k}(1:3) \\ \hat{q} &\Leftarrow \hat{q} \otimes \tilde{q}_e \\ \hat{q} &\Leftarrow \hat{q}/\|\hat{q}\| \\ \hat{x}_{a,k}(1:3) &= 0 \end{aligned} \tag{20}$$

where $\hat{x}_{a,k}(1:3)$ is the first three elements of $\hat{x}_{a,k}$.

- Magnetic sensor measurement update: The standard measurement update algorithm is modified so that only yaw angles are affected by the magnetic sensor measurement update. The explanation of the modified measurement update is given after. Thus

$$\begin{aligned} P_{m,k}^- &= \begin{bmatrix} P_{a,k}(1:3,1:3) & 0_{3,6} \\ 0_{6,3} & 0_{6,6} \end{bmatrix} \\ K_{m,k} &= \begin{bmatrix} r_3 r_3' & 0_{3,6} \\ 0_{6,3} & 0_{6,6} \end{bmatrix} P_{m,k}^- H_{m,k}' \left( H_{m,k} P_{m,k}^- H_{m,k}' + R_m \right)^{-1} \\ \hat{x}_k &= \hat{x}_{a,k} + K_{m,k}(z_{m,k} - H_{m,k}\hat{x}_{a,k}) \\ P_k &= (I - K_{m,k}H_{m,k}) P_{a,k} (I - K_{m,k}H_{m,k})' \\ &\quad + K_{m,k} R_m K_{m,k}' \end{aligned} \tag{21}$$

where $0_{mn}$ is a zero matrix with $m$ rows and $n$ columns, and

$$\begin{aligned} r_3 &= C(\hat{q}) \begin{bmatrix} 0 \\ 0 \\ 1 \end{bmatrix} \\ H_{m,k} &\triangleq \left[\, 2\,[C(\hat{q})\tilde{m}\times] \quad 0 \quad 0 \,\right] \\ z_{m,k} &\triangleq y_{m,k} - C(\hat{q}_k)\tilde{m}. \end{aligned} \tag{22}$$

From the structure of $P_{m,k}^-$ and $K_{m,k}$, we can see that only the $q_e$ part in $\hat{x}_{a,k}$ is updated, i.e., $b_g$ and $b_a$ [see (8)] are not updated in this stage. Thus, we focus our attention to how $C(\hat{q})$ is changed, and it will be shown that only yaw angles are modified in (21). First, consider the following lemma.

*Lemma 1:* Suppose there are two rotation matrices $C_1$ and $C_2$. The pitch and roll angles of $C_1$ and $C_2$ are the same if the following condition is satisfied:

$$(C_1 - C_2) \begin{bmatrix} 0 \\ 0 \\ 1 \end{bmatrix} = 0. \tag{23}$$

*Proof:* See Appendix A.

Note that the rotation matrix before the magnetic sensor measurement update is $C(\hat{q})$, and after the update, it is $C(\bar{q}_e)C(\hat{q})$. From (23), $q_e$ only affects the yaw angle of $C(\hat{q})$ if

$$(C(\bar{q}_e)C(\hat{q}) - C(\hat{q})) \begin{bmatrix} 0 \\ 0 \\ 1 \end{bmatrix} = 0. \tag{24}$$

From (13), the condition (24) can be approximated by [see (22) for the definition of $r_3$]

$$q_e \times r_3 = 0. \tag{25}$$

Thus, $q_e$ only affects the yaw angle if $q_e$ is parallel to $r_3$, i.e.,

$$q_e = \beta r_3, \qquad \beta \in R. \tag{26}$$

Now, we derive a constraint imposed on $K_{m,k}(1:3,1:3)$ so that the updated $q_e$ in (21) satisfies (26). From (20), we have $\hat{x}_{a,k}(1:3) = 0$. Thus, the measurement update equation in (21) is

$$q_e = \hat{x}_k(1:3) = K_{m,k}(1:3,1:3) z_{m,k}. \tag{27}$$

To satisfy (26) for any $z_{m,k}$, $K_{m,k}(1:3,1:3)$ should have the following structure:

$$K_{m,k}(1:3,1:3) = r_3 l' \tag{28}$$

where $l \in R^{1\times 3}$ is a free parameter. We can show (see Appendix B) that a parameter $l$ that minimizes $\mathrm{Tr} P_k(1:3,1:3)$ is given by $l = r_3$. Thus, an optimal filter gain given the constraint (28) is $K_{m,k}$ in (21).

When there are two measurement groups, we obtain the same measurement update result whether the two measurement groups are updated on the same time or each measurement group is updated one at a time as long as appropriate optimal Kalman gains are used (see [6, Ch. 6.3]). Thus, splitting the measurement update into two phases itself does not degrade the estimation performance. However, there is possible estimation performance degradation in the proposed filter since $K_{m,k}$ in (21) is not the optimal Kalman gain: $K_{a,k}$ in (19) is the optimal Kalman gain. A nonoptimal gain $K_{m,k}$ is used so that only the yaw angle is updated in (21). In the process, some information contained in $z_{m,k}$ is intentionally discarded.

## IV. Adaptive Algorithm Compensating External Acceleration

In this section, an adaptive algorithm to estimate external acceleration from the residual is proposed. The residual in the accelerometer measurement update (19) is defined by

$$r_{a,k} \triangleq z_{a,k} - H_{a,k}\hat{x}_k^- = H_{a,k}\left(x_k - \hat{x}_k^-\right) + a_b + v_a.$$

Note that

$$\begin{aligned} \mathrm{E}\left\{r_{a,k} r'_{a,k}\right\} &= \mathrm{E}\left\{\left(z_{a,k} - H_{a,k}\hat{x}_k^-\right)\left(z_{a,k} - H_{a,k}\hat{x}_k^-\right)'\right\} \\ &= H_{a,k} P_k^- H'_{a,k} + Q_{a_b,k} + R_a \end{aligned} \tag{29}$$

where $Q_{a_b,k}$ is the time-varying covariance of the external acceleration $a_b$. In (29), $a_b$ is assumed to be uncorrelated to $H_{a,k}x_k$ and $v_a$. Since $\mathrm{E}\{r_{a,k}r'_{a,k}\}$ cannot be obtained, we use the following approximation:

$$\mathrm{E}\left\{r_{a,k} r'_{a,k}\right\} \approx U_k \triangleq \frac{1}{M_1}\sum_{0}^{M_1-1} r_{a,k-i} r'_{a,k-i}. \tag{30}$$

From (29) and (30), $Q_{a_b,k}$ could be estimated as

$$\hat{Q}_{a_b,k} \approx U_k - \left(H_{a,k}P_k^- H'_{a,k} + R_a\right). \tag{31}$$

One problem of this approach is that $\hat{Q}_{a_b,k}$ is not guaranteed to be nonnegative. Thus, (31) is modified so that $\hat{Q}_{a_b,k} \geq 0$ is guaranteed.

Since $U_k$ is symmetric, there are orthonormal eigenvectors $u_{i,k} \in R^{3\times 1}$ $(i = 1,2,3)$ and corresponding eigenvalues $\lambda_{i,k} \in R$ so that $U_k$ can be expressed as follows:

$$U_k = \sum_{i=1}^{3} \lambda_{i,k} u_{i,k} u'_{i,k}. \tag{32}$$

Let $\mu_{i,k}$ $(i = 1,2,3)$ be defined by

$$\mu_{i,k} \triangleq u'_{i,k}\left(H_{a,k}P_k^- H'_{a,k} + R_a\right) u_{i,k}.$$

Note that $\lambda_{i,k} \geq 0$ and $\mu_{i,k} \geq 0$ since $U_k \geq 0$ and $H_{a,k}P_k^- H'_{a,k} + R_a > 0$. In addition, note that $U_k - (H_{a,k}P_k^- H'_{a,k} + R_a)$ can be expressed as follows:

$$U_k - \left(H_{a,k}P_k^- H'_{a,k} + R_a\right) = \sum_{i=1}^{3}(\lambda_{i,k} - \mu_{i,k}) u_{i,k} u'_{i,k}. \tag{33}$$

An adaptive estimation algorithm of $Q_{a_b,k}$ is given in pseudocode.

- Mode 1 (no external acceleration mode) if $\max_i(\lambda_{i,j} - \mu_{i,j}) < \gamma$ $(j = k, k-1, \ldots, k-M_2)$

$$\hat{Q}_{a_b,k} = 0. \tag{34}$$

- Mode 2 (external acceleration mode) else

$$\hat{Q}_{a_b,k} = \sum_{i=1}^{3} \max(\lambda_{i,k} - \mu_{i,k}, 0) u_{i,k} u'_{i,k}. \tag{35}$$

From (34) and (35), $\hat{Q}_{a_b,k} \geq 0$ is guaranteed, and if $U_k > H_{a,k}P_k^- H'_{a,k} + R_a$, (35) is equivalent to (31). The condition $\max_i(\lambda_{i,j} - \mu_{i,j}) < \gamma$ is introduced so that (35) is only used when $U_k$ is significantly greater than $H_{a,k}P_k^- H'_{a,k} + R_a$ in any directions. This is to prevent $\hat{Q}_{a_b,k}$ from being affected by normal fluctuation of accelerometer noises. $M_2$ is introduced so that transition from mode 2 to mode 1 occurs only if $\max_i(\lambda_{i,j} - \mu_{i,j}) < \gamma$ is satisfied for $M_2 + 1$ consecutive times. This is to prevent falsely entering mode 1 when there is external acceleration. There is no delay in transition from mode 1 to mode 2, so that external acceleration is quickly estimated.

How accurately can $Q_{a_b,k}$ be estimated? From (31), we can see the accuracy of $\hat{Q}_{a_b,k}$ depends on $H_{a,k}$, $P_k^-$, and $R_a$. The state estimation error $P_k^-$ is usually the largest at the initial time and tends to decrease until it converges to some values. In particular, bias estimation is not accurate immediately after the initial time. Thus, accurate estimation of $Q_{a_b,k}$ is rather difficult immediately after the initial time. As shown in Section V, sensor biases can be estimated after a few minutes, and after that, the sensor bias effect on $\hat{Q}_{a_b,k}$ is small.

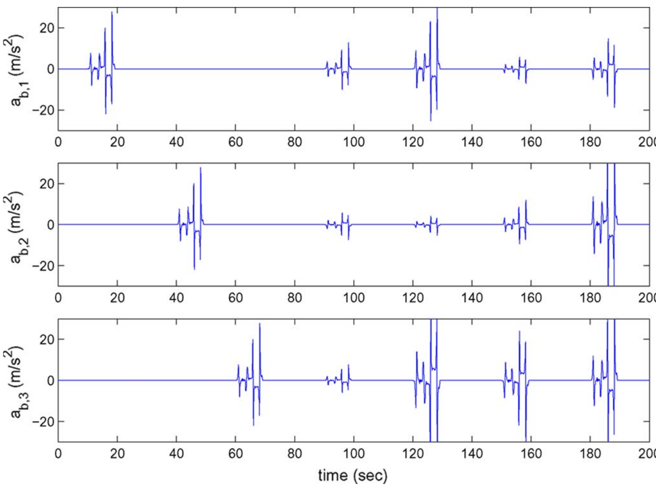


Fig. 2. External acceleration $a_b$.

## V. Numerical Examples

To verify the proposed algorithm, two sets of data are used: one is data generated by MATLAB, and the other is real sensor data.

In the first data, external acceleration in Fig. 2 is used. Parameters used for the first data are as follows:

$$\begin{aligned} &R_a = 0.0056I \quad && R_g = 0.003I \quad && R_m = 0.001I \\ &Q_{b_g} = 0.000001I \quad && Q_{b_a} = 0.000001I && \\ &M_1 = 3 && M_2 = 2 && \gamma = 0.1. \end{aligned} \tag{36}$$

We applied three filters, where all three filters have the same quaternion-based indirect Kalman filter structure used in this paper. The difference only lies in the adaptive algorithm part $\hat{Q}_{a_b}$. The first filter is the standard Kalman filter, where no adaptive algorithm is used (i.e., $\hat{Q}_{a_b} = 0$ all the time). The second filter is an accelerometer norm-based adaptive algorithm [11], i.e.,

$$\hat{Q}_{a_b,k} = \begin{cases} 0, & |\|y_{a,k}\|_2 - 9.8| < 0.2 \\ sI, & \text{otherwise} \end{cases} \tag{37}$$

where $s \in R$ is a constant. In [11], $s = \infty$ is used, and in this paper, three different values (1, 10, 100) are used. The third filter is the proposed adaptive filter.

The results are given in Table I, where three filters are tested with 100 randomly generated data. In the three filters, a quaternion is computed, and it is transferred to Euler angles for visual comparison. We can see that the proposed adaptive filter provides significantly better results. One example of orientation estimation by the proposed filter is given in Fig. 3. Gyroscope and accelerometer bias estimation results are given in Figs. 4 and 5, respectively. To see bias estimation ability, averages and variances of $b_g - \hat{b}_g$ and $b_a - \hat{b}_a$ (at 200 s) for the 100 experiments are given in Table II.

TABLE I
Average Estimation Error of 100 Experiments
($e_\phi \triangleq \phi - \hat{\phi}$, $e_\theta \triangleq \theta - \hat{\theta}$, $e_\psi \triangleq \psi - \hat{\psi}$, Ave$\{e_k^2\} \triangleq (1/N) \sum_{k-1}^{N} e_k^2$)

| | Ave$\{e_{\phi,k}^2\}$ | Ave$\{e_{\theta,k}^2\}$ | Ave$\{e_{\psi,k}^2\}$ |
|---|---|---|---|
| standard Kalman filter | 556.2 | 142.9 | 625.3 |
| accelerometer norm-based adaptive filter ($s = 1$) | 69.3 | 14.0 | 90.6 |
| accelerometer norm-based adaptive filter ($s = 10$) | 50.1 | 9.0 | 63.7 |
| accelerometer norm-based adaptive filter ($s = 100$) | 54.5 | 10.0 | 71.7 |
| proposed adaptive filter | 15.8 | 2.5 | 16.9 |

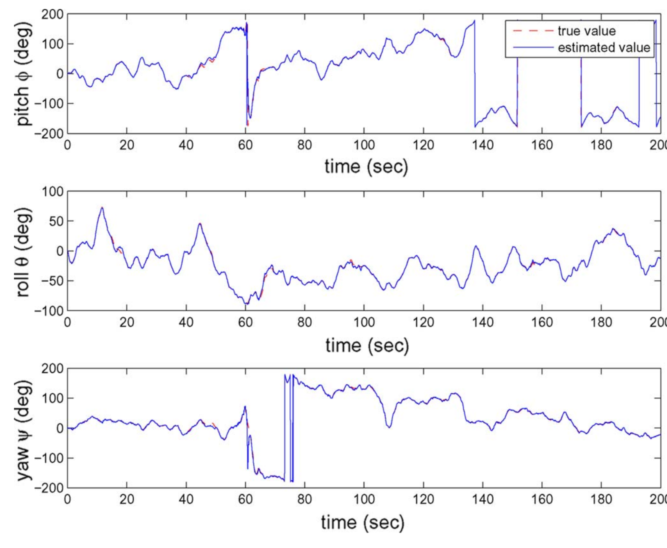


Fig. 3. Orientation estimation by the proposed filter.

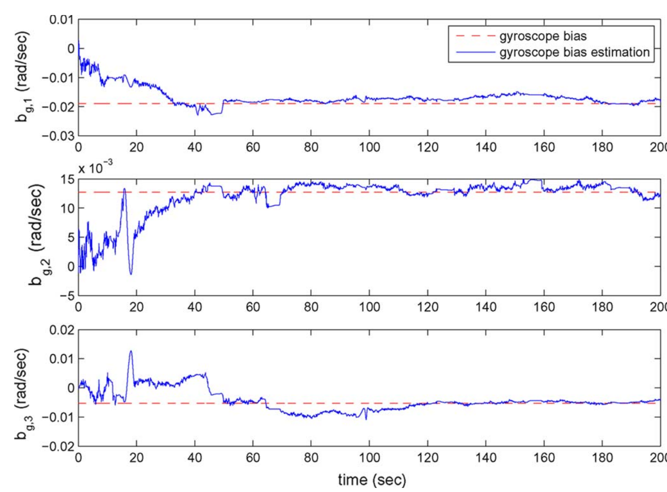


Fig. 4. Gyroscope bias estimation.

To give some insight about the proposed filter, we consider an orientation estimation problem, where external acceleration is given only in the $x$-axis, as shown in Fig. 6. The parameters used are the same as (36), except for the bias, where $b_g = b_a = 0$ are assumed. The results are given in Figs. 7–9 and Table III. It can be seen that both adaptive filters are robust with respect to external acceleration compared with the standard Kalman filter.

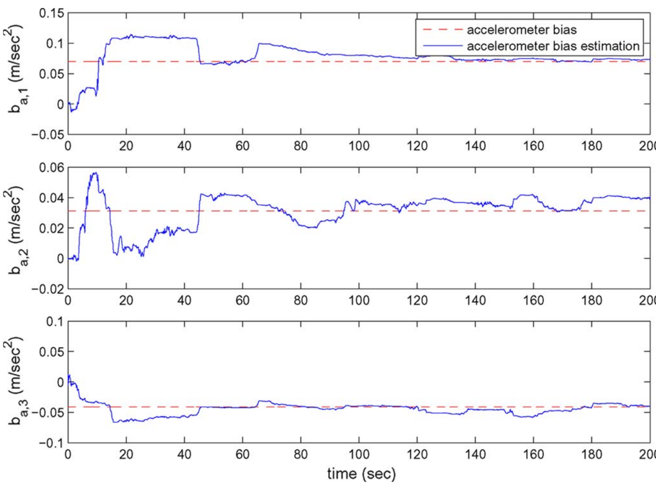


Fig. 5. Accelerometer bias estimation.

TABLE II
BIAS ESTIMATION RESULT FOR 100 EXPERIMENTS (AT 200 s)

| | variance | average |
|---|---|---|
| $b_{g,1} - \hat{b}_{g,1}$ | $3.3 \times 10^{-6}$ | $1.4 \times 10^{-4}$ |
| $b_{g,2} - \hat{b}_{g,2}$ | $3.9 \times 10^{-6}$ | $1.3 \times 10^{-4}$ |
| $b_{g,3} - \hat{b}_{g,3}$ | $3.7 \times 10^{-6}$ | $2.5 \times 10^{-4}$ |
| $b_{a,1} - \hat{b}_{a,1}$ | $9.6 \times 10^{-5}$ | $-1.3 \times 10^{-3}$ |
| $b_{a,2} - \hat{b}_{a,2}$ | $1.1 \times 10^{-4}$ | $7.2 \times 10^{-4}$ |
| $b_{a,3} - \hat{b}_{a,3}$ | $9.6 \times 10^{-5}$ | $-2.5 \times 10^{-3}$ |

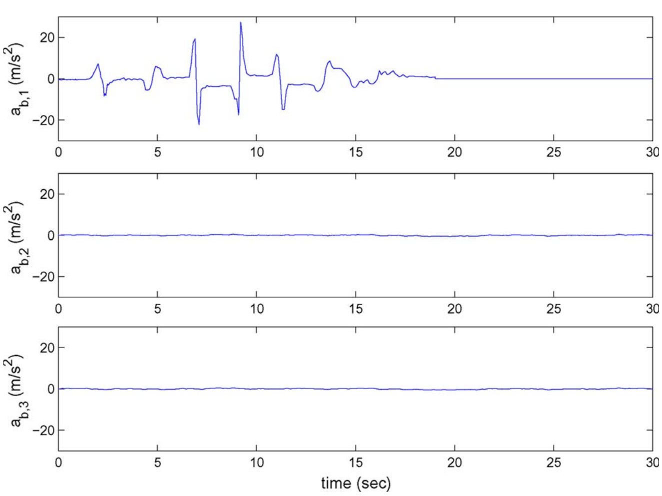


Fig. 6. External acceleration $a_b$.

The difference between the two adaptive filters are explained. Note that the $x$-axis external acceleration affects mostly the roll angle estimation since the roll angle is determined by the ratio between the $x$- and $z$-axis accelerometer output. In the accelerometer norm-based filter, $\hat{Q}_{a_b} = sI$ as in (37) when external acceleration is detected: note that choosing $\hat{Q}_{a_b} = sI$ is equivalent to giving less weights to all three-axis accelerometer output. In this example, external acceleration is only applied to the $x$-axis, and by giving less weights on the $y$- and $z$-axis accelerometer output (with respect to the gyroscope integrated

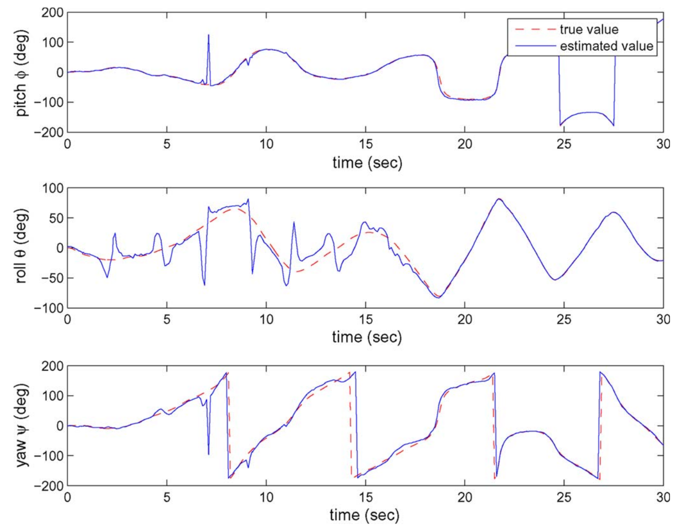


Fig. 7. Standard Kalman filter.

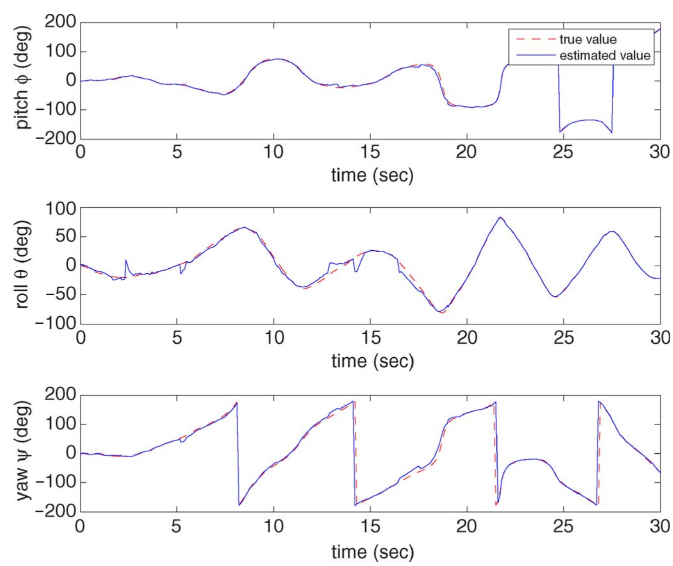


Fig. 8. Accelerometer norm-based adaptive filter $(s = 10)$.

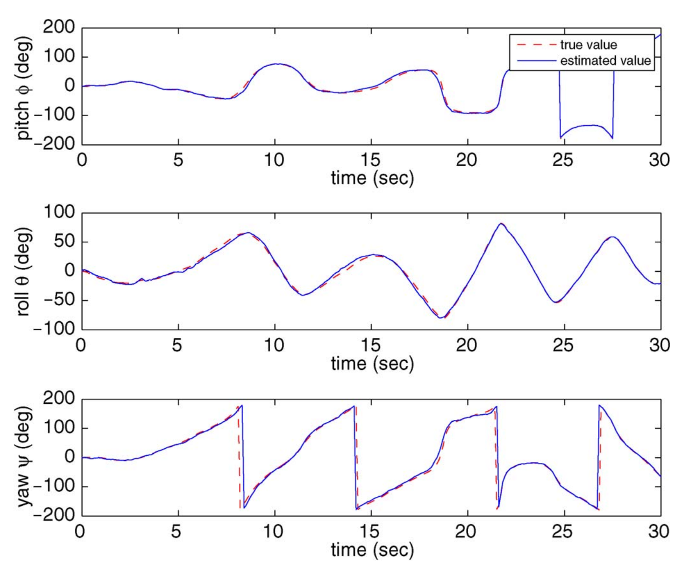


Fig. 9. Proposed filter.

TABLE III
AVERAGE ESTIMATION ERROR OF 100 EXPERIMENTS

| | $\text{Ave}\{e_{\phi,k}^2\}$ | $\text{Ave}\{e_{\theta,k}^2\}$ | $\text{Ave}\{e_{\psi,k}^2\}$ |
|---|---|---|---|
| standard Kalman filter | 110.0 | 258.4 | 186.3 |
| accelerometer norm-based adaptive filter ($s = 1$) | 25.7 | 33.8 | 54.4 |
| accelerometer norm-based adaptive filter ($s = 10$) | 42.9 | 28.7 | 60.7 |
| accelerometer norm-based adaptive filter ($s = 100$) | 67.0 | 30.8 | 80.7 |
| proposed adaptive filter | 32.5 | 8.4 | 33.9 |

value), useful information in the $y$- and $z$-axis accelerometer output is lost. On the other hand, $\hat{Q}_{a_b}$ is adaptively estimated as in (35). For example, at time 7.3 s, $\hat{Q}_{a_b}$ is given by

$$\hat{Q}_{a_b} = \begin{bmatrix} 8.8172 & -0.4637 & 0.8861 \\ -0.4637 & 0.0244 & -0.0466 \\ 0.8861 & -0.0466 & 0.0891 \end{bmatrix}. \quad (38)$$

We can see that only the $x$-direction element of $\hat{Q}_{a_b}$ is increased, and thus, the $y$- and $z$-axis accelerometer information is not lost.

See Table III for a quantitative comparison of the two adaptive filters. See how the performance of the accelerometer norm-based adaptive filter is changed with respect to the value of $s$. When $s = 1$, pitch angle estimation is good, but roll estimation is not good compared with the $s = 100$ case. By taking small $s$ values, the $y$-axis element of $\hat{Q}_{a_b}$ becomes small, and thus, the $y$-axis accelerometer information is used more compared with the $s = 100$ case. The price paid is that the $x$-axis element of $\hat{Q}_{a_b}$ becomes also small and the filter becomes sensitive to $x$-axis external acceleration. In the accelerometer norm-based adaptive algorithm, there is a fundamental tradeoff between robustness to external acceleration and use of the nonexternal-acceleration-direction accelerometer output. In the proposed filter, by estimating the direction of external acceleration, we can achieve both objectives: robust to external acceleration while using the nonexternal-acceleration-direction accelerometer output.

Detection abilities of external acceleration of the two adaptive filters are given in Fig. 10, where both filters show similar detection abilities.

In the second example, real sensor data are used, where an inertial/magnetic sensor unit MTi from a company XSENS is used. We used the same filter parameters (36) for the second example. A sensor unit is rotated back and forth with a hand almost periodically. A magnet is placed near the sensor from 16 to 21 s to generate magnetic disturbance. The magnetic sensor output is given in Fig. 11, where disturbance due to the magnet can be seen between 16 and 21 s. The accelerometer norm-based adaptive filter result is given in Fig. 12, where the magnetic sensor output is used to estimate pitch, roll, and yaw angles. We can see that magnetic disturbance affects not only the yaw angle but also the pitch and roll angles. The proposed two-step filter result is given in Fig. 13. It can be seen that the pitch and roll angles are not affected by magnetic disturbances.

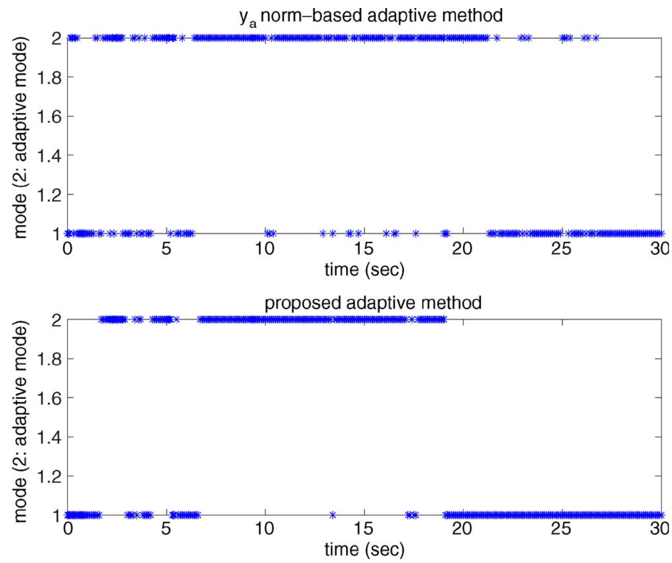


Fig. 10. External acceleration detection. (Top) Accelerometer norm-based detection (37). (Bottom) Proposed detection (34).

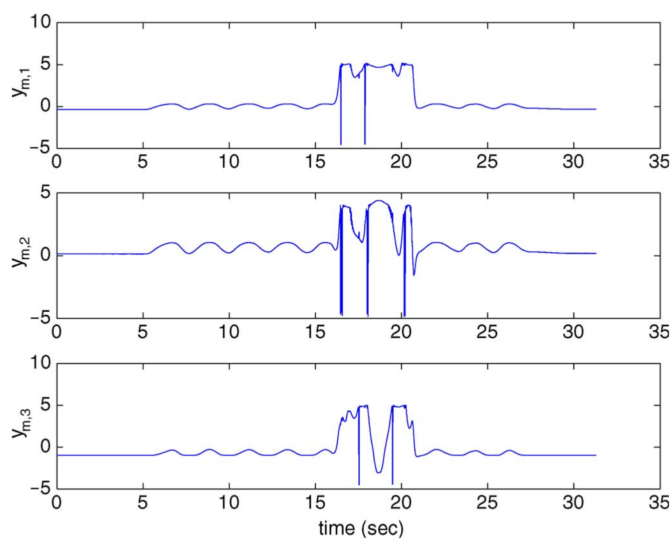


Fig. 11. Magnetic sensor output $y_m$ (arbitrary unit).

## VI. CONCLUSION

An adaptive orientation filter has proposed to compensate external acceleration. In conventional accelerometer norm-based adaptive algorithms, small weights are given to all three-axis accelerometer values when external acceleration is detected. Thus, orientation estimation mostly depends on gyroscope integration. In the proposed filter, the direction of external acceleration is estimated ($\hat{Q}_{a_b}$), and small weights are only given to accelerometer values affected by external acceleration, whereas accelerometer values not affected are still used along with gyroscope integration. Thus, the proposed method uses more information for orientation estimation and provides a better result with respect to external acceleration. One limitation of this paper is that the magnetic disturbances are not adaptively compensated, and this is one of future topics.

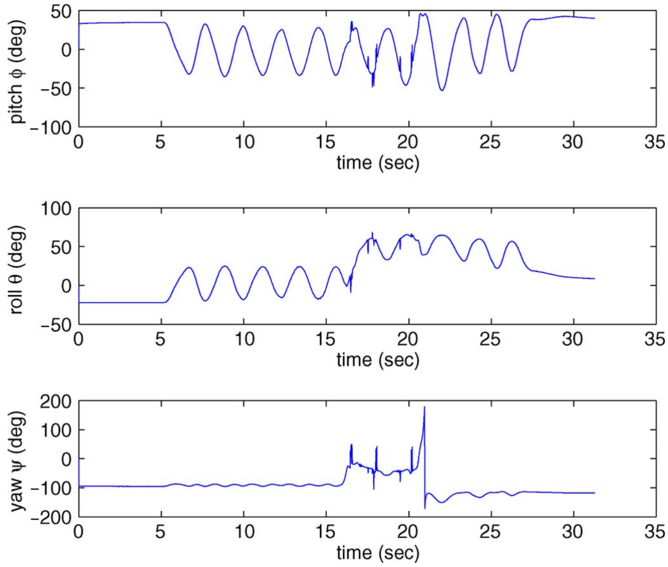


Fig. 12. Accelerometer norm-based adaptive filter (the magnetic sensor output is used to estimate pitch, roll, and yaw angles).

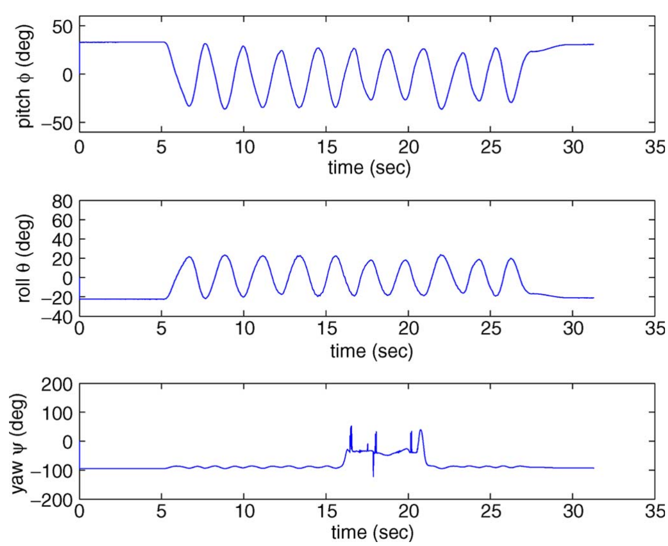


Fig. 13. Proposed filter (the magnetic sensor output is only used to estimate the yaw angle).

## APPENDIX A

Let $[\phi \quad \theta \quad \psi]'$ be Euler angles usually defined in aerospace applications [4]: the first rotation is about the $z$-axis through an angle $\psi$ (yaw angle), the second is about the $y$-axis through an angle $\theta$, and the third is about the $z$-axis through an angle $\phi$. When the Euler angles are $[\phi \quad \theta \quad \psi]'$, the corresponding rotation matrix $C$ is given by

$$\begin{bmatrix} \mathrm{c}\,\theta\,\mathrm{c}\,\psi & \mathrm{c}\,\theta\,\mathrm{s}\,\psi & -\mathrm{s}\,\theta \\ \mathrm{s}\,\phi\,\mathrm{s}\,\theta\,\mathrm{c}\,\psi - \mathrm{c}\,\phi\,\mathrm{s}\,\psi & \mathrm{s}\,\phi\,\mathrm{s}\,\theta\,\mathrm{s}\,\psi + \mathrm{c}\,\phi\,\mathrm{c}\,\psi & \mathrm{s}\,\phi\,\mathrm{c}\,\theta \\ \mathrm{c}\,\phi\,\mathrm{s}\,\theta\,\mathrm{c}\,\psi + \mathrm{s}\,\phi\,\mathrm{s}\,\psi & \mathrm{c}\,\phi\,\mathrm{s}\,\theta\,\mathrm{s}\,\psi - \mathrm{s}\,\phi\,\mathrm{c}\,\psi & \mathrm{c}\,\phi\,\mathrm{c}\,\theta \end{bmatrix} \tag{39}$$

where $\mathrm{s}\phi$ means $\sin\,\phi$, and $\mathrm{c}\phi$ means $\cos\,\phi$.

*Proof of Lemma 1:* From (39), $\phi$ (pitch) and $\theta$ (roll) of $C_1$ and $C_2$ are the same if the third columns of $C_1$ and $C_2$ are the same. Thus. the pitch and roll angles of $C_1$ and $C_2$ are the same if (23) is satisfied. ■

## APPENDIX B

For simplicity, we define symbols $\tilde{K}$, $\tilde{P}$, $\tilde{P}_a$, and $\tilde{H}$ as

$$\begin{aligned} \tilde{K} &= K_{m,k}(1:3,1:3) \\ \tilde{P} &= P_k(1:3,1:3) \\ \tilde{P}_a &= P_{a,k}(1:3,1:3) \\ \tilde{H} &= H_{m,k}(1:3,1:3). \end{aligned}$$

Then, from the last equation of (21), we have

$$\tilde{P} = (I - \tilde{K}\tilde{H})\tilde{P}_a(I - \tilde{K}\tilde{H})' + \tilde{K}R_m\tilde{K}'. \tag{40}$$

Suppose $\tilde{K}$ satisfies (28), i.e., $\tilde{K} = r_3 l'$, where $l$ is a free parameter. We want to find a parameter $l$ that minimizes $\mathrm{Tr}\,\tilde{P}$. Invoking the fact $\mathrm{Tr}AB = \mathrm{Tr}BA$, we have

$$\mathrm{Tr}\,\tilde{P} = \mathrm{Tr}\,C(\hat{q})C'(\hat{q})\tilde{P} = \mathrm{Tr}\,C'(\hat{q})\tilde{P}C(\hat{q}) = \sum_{i=1}^{3} r_i'\tilde{P}r_i \tag{41}$$

where

$$r_1 = C(\hat{q})\begin{bmatrix}1\\0\\0\end{bmatrix} \qquad r_2 = C(\hat{q})\begin{bmatrix}0\\1\\0\end{bmatrix}.$$

From (40) and (41), we have

$$\mathrm{Tr}\,\tilde{P} = \sum_{i=1}^{3} r_i'\left((I - r_3 l'\tilde{H})\tilde{P}_a(I - r_3 l'\tilde{H})' + r_3 l' R_m l r_3'\right) r_i.$$

Noting that

$$r_i r_j' = \begin{cases} 1, & i = j \\ 0, & i \neq j \end{cases}$$

we have

$$\mathrm{Tr}\,\tilde{P} = l'\tilde{H}\tilde{P}_a\tilde{H}'l' + r_3'\tilde{P}_a\tilde{H}'l + l'\tilde{H}\tilde{P}_a r_3 + l'R_m l + \star$$

where $\star$ denotes all terms not containing the parameter $l$. Thus, minimizing $l$ can be found from the following minimization problem:

$$\min_{l}\; l'\tilde{H}\tilde{P}_a\tilde{H}'l' + r_3'\tilde{P}_a\tilde{H}'l + l'\tilde{H}\tilde{P}_a r_3 + l'R_m l.$$

Completing the square, we obtain the optimal $l$, i.e.,

$$l = r_3'\tilde{P}_a\tilde{H}'(\tilde{H}\tilde{P}\tilde{H}' + R_m)^{-1}.$$

Inserting this $l$ into (28), we obtain (21).

## REFERENCES


[1] G. Welch and E. Foxlin, "Motion tracking: No silver bullet, but a respectable arsenal," *IEEE Comput. Graph. Appl.*, vol. 22, no. 6, pp. 24–38, Nov./Dec. 2002.

[2] S. A. Salman, A. G. Sreenatha, and J. Y. Choi, "Attitude dynamics identification of unmanned aircraft vehicle," *Int. J. Control Autom. Syst.*, vol. 4, no. 6, pp. 782–787, 2006.

[3] A. M. Sabatini, C. Martelloni, S. Scapellato, and F. Cavallo, "Assessment of walking features from foot inertial sensing," *IEEE Trans. Biomed. Eng.*, vol. 52, no. 3, pp. 486–494, Mar. 2005.

[4] J. B. Kuipers, *Quaternions and Rotation Sequences: A Primer With Applications to Orbits, Aerospace, and Virtual Reality*. Princeton, NJ: Princeton Univ. Press, 1999.

[5] W. F. Phillips and C. E. Hailey, "Review of attitude representations used for aircraft kinematics," *J. Aircr.*, vol. 38, no. 4, pp. 718–737, Jul./Aug. 2001.

[6] R. G. Brown and P. Y. C. Hwang, *Introduction to Random Signals and Applied Kalman Filtering*. New York: Wiley, 1997.

[7] E. Foxlin, "Inertial head-tracker sensor fusion by a complementary separate-bias Kalman filter," in *Proc. IEEE Virtual Reality Annu. Int. Symp.*, 1996, pp. 185–194.

[8] E. J. Lefferts, F. L. Markley, and M. D. Shuster, "Kalman filter for spacecraft attitude estimation," in *Proc. AIAA 20th Aerosp. Sci. Meeting*, 1982, pp. 1–16.

[9] C. Creamer, "Spacecraft attitude determination using gyros and quaternion measurements," *J. Astronaut. Sci.*, vol. 44, no. 3, pp. 357–371, 1996.

[10] J. K. Hall, N. B. Knoebel, and T. W. McLain, "Quaternion attitude estimation for miniature air vehicles using a multiplicative extended Kalman filter," in *Proc. IEEE Position, Location Navig. Symp.*, 2008, pp. 1230–1237.

[11] A. M. Sabatini, "Quaternion-based extended Kalman filter for determining orientation by inertial and magnetic sensing," *IEEE Trans. Biomed. Eng.*, vol. 53, no. 7, pp. 1346–1356, Jul. 2006.

[12] X. Yun and E. R. Bachmann, "Design, implementation, and experimental results of a quaternion-based Kalman filter for human body motion tracking," *IEEE Trans. Robot.*, vol. 22, no. 6, pp. 1216–1227, Dec. 2006.

[13] X. Yun, E. R. Bachmann, and R. B. McGhee, "A simplified quaternion-based algorithm for orientation estimation from earth gravity and magnetic field measurements," *IEEE Trans. Instrum. Meas.*, vol. 57, no. 3, pp. 638–650, Feb. 2008.

[14] R. Zhu and Z. Zhou, "A small low-cost hybrid orientation system and its error analysis," *IEEE Sensors J.*, vol. 9, no. 3, pp. 223–230, Mar. 2009.

[15] Y. S. Suh, S. K. Park, H. J. Kang, and Y. S. Ro, "Attitude estimation adaptively compensating external acceleration," *JSME Int. J. Ser. C*, vol. 49, no. 1, pp. 172–179, 2006.

[16] J. K. Lee and E. J. Park, "A minimum-order Kalman filter for ambulatory real-time human body orientation tracking," in *Proc. IEEE Int. Conf. Robot. Autom.*, 2009, pp. 3565–3570.

[17] P. S. Maybeck, *Stochastic Models, Estimation, and Control*. New York: Academic, 1982.

[18] E. Bekir, *Introduction to Modern Navigation Systems*. Singapore: World Scientific, 2007.

[19] R. P. Collinson, *Introduction to Avionics Systems*, 2nd ed. Berlin, Germany: Springer-Verlag, 2003.

[20] E. R. Bachmann, X. Yun, and A. Brumfield, "Investigating the effects of magnetic variations on inertial/magnetic orientation sensors," *IEEE Robot. Autom. Mag.*, vol. 14, no. 3, pp. 76–87, Sep. 2007.

[21] M. Shuster and S. Oh, "Three-axis attitude determination from vector observations," *J. Guid. Control*, vol. 4, no. 1, pp. 70–77, Jan./Feb. 1981.

**Young Soo Suh** (M'90) received the B.S. and M.S. degrees from Seoul National University, Seoul, Korea, in 1990 and 1992, respectively, and the Ph.D. degree from The University of Tokyo, Tokyo, Japan, in 1997.

He is currently a Professor with the Department of Electrical Engineering, University of Ulsan, Ulsan, Korea. His research interests include networked control systems and attitude estimation and control, and personal navigation systems.